Mapping lipid C=C isomer profiles of human gut bacteria by a novel structural lipidomics workflow assisted by chemical epoxidation

Kai-Li Chen, [†,‖] Ting-Hao Kuo,[†,‡,‖] ,and Cheng-Chih Hsu[†,*]

† Department of Chemistry, National Taiwan University, Taipei, Taiwan.

‡ European Molecular Laboratory, Heidelberg, Germany.

ABSTRACT: The unsaturated lipids produced by human gut bacteria exhibit extraordinary structural diversity, largely attributed to the isomerism of the carbon-carbon double bond (C=C) in terms of position and stereochemistry. Characterizing these distinct C=C configurations poses a significant challenge in the research field, primarily due to limitations in current bioanalytical methodologies. In this study, we developed a novel structural lipidomic workflow by integrating an epoxidation protocol using meta-chloroperoxybenzoic acid for C=C derivatization and liquid chromatography-tandem mass spectrometry for C=C characterization. We utilized this workflow to quantitatively assess over 50 C=C positional and *cis/trans* isomers of fatty acids and phospholipids from selected human gut bacteria. The strain-specific isomer profiles revealed unexpected and remarkable productivity of trans-10-octadecenoic acid by Enterococcus faecalis, Bifidobacterium longum, and Lactobacillus acidophilus, among numerous other trans fatty acid isomers produced by gut bacteria. Isotope-tracking experiments suggest that gut bacteria produce trans-10-octadecenoic acid through isomeric biotransformation of oleic acid in vitro and that such isomeric biotransformation of dietary oleic acid is dependent on the presence of gut bacteria in vivo.

INTRODUCTION

The human gastrointestinal tract harbors a vast microbial community involving trillions of bacterial cells, known as the gut microbiota [1]. These bacteria actively engage in metabolic activities, producing a wide array of small-molecule chemical products, called metabolites, that profoundly influence various aspects of human physiology [2-6]. The complex metabolic processes within the gut bacterial community involve biochemical interactions with both ingested compounds[7] and the human host[8], as well as bacterial cellular de novo synthesis[9]. Over the past decade, extensive characterization of gut bacterial metabolites has revealed their diverse functional roles, such as immune responses[10] and disease biomarkers[11], and neurological signaling[12]. Moreover, recent research on biotransformation, one of the mechanisms by which these metabolites are produced, has further elucidated the overarching impacts of gut bacterial metabolism on drug availability and efficacy[13]. The diversity of gut bacterial metabolites and the significance of gut biotransformation have catalyzed a thriving research area, illuminating the intricate connection between gut bacterial metabolism and human health.

Gut bacterial lipids are one of the important gut bacterial metabolites. They play different roles in the interaction between gut bacteria and host[14] such as energy homeostasis[15] and regulation of inflammation[16]. Among the lipid metabolites, unsaturated lipid, i.e. lipid metabolites containing carbon-carbon double bonds (C=C) on their fatty acyl chains, is a main class of lipid metabolites with diverse structure and biological functions[17]. Unsaturated lipids are produced from bacteria by de novo synthesis and biotransformation[18, 19]. Unlike mammalian unsaturated lipids, little has been known about gut bacterial precise unsaturated lipids' chemical structure and biological function, which may be due to their diverse structures and unclear biotransformation pathway. As a result, characterizing the gut bacterial unsaturated lipid structures including the C=C position and geometry is a key to investigate the function and activities of these metabolites.

In recent years, mass spectrometry has become a powerful tool in lipidomics because it can provide high-throughput, highly sensitive, and rapid analysis of lipid molecules in biological samples[20, 21]. However, the structural information of unsaturated lipids, especially C=C position and geometry which are key factors determining unsaturated lipid structure, chemical properties, and bioactivity[7, 22-26], cannot be obtained by conventional tandem mass spectrometry[20, 27]. To address this challenge, several MS-based methods have been developed. For example, electron impact excitation of ions from organics (EIEIO)[28], ultraviolet photodissociation (UVPD)[29], hydrogen abstraction dissociation (HAD)[30], and radical-directed dissociation[31] utilized special fragmentation methods to break down C=C to identify C=C position by MS^n spectrum. Other ways that coupling derivatization of C=C double bonds with mass spectrometry such as Paternò–Büchi (PB) reaction[32], epoxidation[33, 34], ozonolysis[35, 36], aziridination[37] and thio-ene reaction[38] turned C=C structure into other more unstable structures so that the C=C position can be determined from products MS^n spectra. Although the above methods successfully help determine C=C position, the C=C geometry was still not resolved effectively due to the similar MS^n spectra of geometric isomers. To distinguish geometric isomers, coupling mass spectrometry with separation method such as chromatography[39] and ion mobility[40, 41] is a possible solution. For examples, GC-MS can separate C=C isomers of fatty acid methyl ester and identify them by retention time[42]. Besides, Xie, X.-B. and Xia, Y. identified conjugated fatty acids C=C geometric isomers with trapped ion mobility mass spectrometry[43] which determine the C=C geometry by the drift time. Recently, Feng, G.-F. et al. established a method that combines photocycloaddition-photoisomerization reaction and

liquid chromatography tandem mass spectrometry, which enable the characterization of either C=C position or geometry without lipid standards[44]. Nevertheless, these methods may face significant challenges when defining both C=C position and geometry for multiple unsaturated lipid species in a routine lipidomics experiment.

Herein we presented a novel methodology in structural lipidomics to characterize C=C position and geometry. Technically, the method integrates reversed-phase liquid chromatography-tandem mass spectrometry (RPLC-MS/MS) with lipid derivatization by *m*CPBA epoxidation and facilitates the characterization of C=C position and geometry in a routine lipidomics experiment. The quantitative and qualitative capability were validated systematically with authentic chemical standards of lipid isomers. To demonstrate its utility, we applied the method in investigating the lipid extracts from gut bacteria and mice feces. Interestingly, we found a gut bacteria-related *cis-trans* isomerization and showed the effect of gut bacteria on C=C isomerism.

MATERIAL AND METHOD

Chemicals and reagents

Fatty acid (FA) standards were purchased from Cayman Chemical (Michigan, USA) except that FA18:1 (10E) was purchased from Life lipid (California, USA). Glycerophospholipid (GPL) standards were purchased from Avanti Polar Lipids (Alabaster, AL, USA). Methanol was purchased from Duksan Pure Chemical (Seonggok-dong, Korea), and methyl tert-butyl ether (MTBE) was purchased from Alfa Aesar (Massachusetts, United States). meta-Chloroperoxybenzoic acid (*m*CPBA) and ammonium acetate were purchased from Sigma Aldrich (St. Louis, USA). 2-Propanol (IPA) was purchased from Honeywell (Michigan, USA). Acetonitrile (ACN) was purchased from J.T. Baker (New Jersey, USA). Ultrapure water (18.2 M Ω) was prepared by a PURELAB Classic system (ELGA, Buckinghamshire, United Kingdom). Tryptic soy agar (TSA) with 5 % sheep blood agar plate was purchased from Dr. Plate (Taipei, Taiwan). MRS medium was purchased from NEOGEN (Michigan, USA).

Lipid nomenclature

The lipid nomenclature reported by Liebisch G. et al. was adopted in the study[45]. FA 18:1 (9Z) represents a fatty acid with 18 carbon atoms and 1 double bond on the ninth carbon in Z-configuration. The double bond position was annotated according to Δ-nomenclature if the configuration was yet to be characterized (e.g., FA18:1 (Δ9)). For phospholipid, the slash was used when the sn-position of acyl chains was identified (e.g., PG 18:0/16:0), whereas the underscore was used when the sn-position of acyl chains was unknown (e.g., PG 18:0 16:0).

Protocol of lipid C=C derivatization by *m*CPBA

The lipid derivatization reagent was prepared by dissolving 44.8 mg *m*CPBA powder in 1 mL methanol to reach a final *m*CPBA concentration of 200 mM. A lipid sample (lipid standard or biological extract) was added with an equal volume of the derivatization reagent, incubated for 1 hour at 50°C, and analyzed by mass spectrometry. The epoxidation protocol was modified from our previous study. Liquid-chromatography mass spectrometry analysis.

Instrumental parameters

All LC-MS experiments were performed using an Orbitrap Elite Mass Spectrometer (Thermo Scientific,Massachusetts, USA) coupled with Thermo Vanquish UHPLC (Thermo Scientific, Massachusetts, USA). A heated electrospray ionization (HESI) probe was equipped as the ionization source with the following parameters: spray voltage at 3.5 kV in negative ionization mode; capillary temperature at 320°C; HESI heater temperature at 250°C; sheath gas flow at 25 (A.U.) and auxiliary gas at 10 (A.U.); the ion optics were tuned at *m/z* 283.26 ([M-H]− ion of FA 18:0). The liquid chromatography was performed using 1.7 μm Waters Acquity CSH C18 column (100 × 2.1 mm, Waters, Massachusetts, USA). A binary gradient was performed with mobile phase A of ACN/water (40/60, v/v) and mobile phase B of IPA/ACN (90/10, v/v). Both A and B solvents contain 10.0 mM ammonium acetate. The optimized 30-min gradient was established as 0-3min, 20 %B; 3-10min, 20 30 %B; 10-15min, 30 50 %B; 15-21min, 50 99 %B; 21-24min 99 %B; 24-26min, 99 20 %B, 26-30min, 20 %B

Targeted lipid analysis of the lipid standards

A lipid standards mixture containing 14 monounsaturated fatty acid C=C isomers was prepared. The standards used included: FA 16:1 (7Z), FA 16:1 (9Z), FA 16:1 (9E), FA 16:1 (11Z), FA 16:1, (11E), FA 18:1 (6Z), FA 18:1 (6Z), FA 18:1 (8Z), FA 18:1 (9Z), FA 18:1 (9E), FA 18:1 (11Z), FA 18:1 (11E), FA 20:1 (11Z), and FA 20:1 (11E). The concentration of each isomer ranged from 0.1 μM to 10 μM. Then the mixture was epoxidated by the addition of an equal volume of 200 mM *m*CPBA. For targeted unsaturated fatty acid C=C isomers analysis, a targeted MS/MS method was established. The scanning cycle consists of one full FT-MS scanning with a mass range of 200-2000 and spectral resolution of 60000, followed by 5 targeted IT-MS/MS scanning events. The MS/MS spectra of 5 targeted epoxy-precursor ions, FA 16:1 (*m/z* = 269.20), FA17:1 (*m/z* =283.30), FA 18:1 (*m/z* =297.24), FA 19:1 (*m/z* = 311.26), FA 20:1 (*m/z* = 325.28), were acquired via ion activation type of CID, isolation width of *m/z* 2.0, normalized collision energy (NCE) of 40.0, activation Q of 0.250, and activation time of 10.00 ms. The maximum injection time for both full FT-MS and IT MS^n was set at 500 ms with auto-gain-control (AGC) of 1.00e+6 for full FT-MS scan and 3.00e+4 for IT MS/MS. The data was collected with Xcalibur 3.0 (Thermo Scientific).

Targeted unsaturated fatty acid C=C isomers analysis of the gut bacterial lipid extracts

For targeted unsaturated fatty acid C=C isomers analysis, a targeted MS/MS method was established. The scanning cycle consists of one full FT-MS scanning with a mass range of 100-1000 and spectral resolution of 60000, followed by 5 targeted IT-MS/MS scanning events. The MS/MS spectra of 5 targeted epoxy-precursor ions, FA 16:1 (*m/z* = 269.21), FA17:1 (*m/z* =283.22), FA18:1 (*m/z* =297.24), FA19:1 (*m/z* = 311.25), FA20:1 (*m/z* = 325.27), were acquired via ion activation type of CID, isolation width of *m/z* 1.0, normalized collision energy (NCE) of 40.0, activation Q of 0.250, and activation time of 10.00 ms. The maximum injection time for both full FT-MS and IT MS^n was set at 500 ms with auto-gain-control (AGC) of 1.00e+6 for full FT-MS scan and 3.00e+4 for IT MS/MS. The data was collected with Xcalibur 3.0 (Thermo Scientific).

Gut bacterial isotope tracking analysis

A targeted MS/MS method was established for gut bacterial isotope tracking analysis. The scanning cycle consists of one full FT-MS scanning with a mass range of 100-1000 and spectral resolution of 60000, followed by 6 IT-MS/MS scanning events. The MS/MS spectra of 6 targeted epoxy-

precursor ions, FA 16:1 (*m/z* = 269.25), FA 17:1 (*m/z* = 283.25), FA 18:1 (*m/z* =297.80), FA 19:1 (*m/z* = 311.30), FA 20:1 (*m/z* = 325.30), and D_{17}-FA 18:1 (*m/z* = 314.30), were acquired via ion activation type of CID, isolation width of *m/z* 2.0, NCE of 40, activation Q of 0.250, and activation time of 10.00 ms. The maximum injection time for both full FT-MS and IT MS^n was set at 500 ms with auto-gain-control (AGC) of 1.00e+6 for full FT-MS scan and 3.00e+4 for IT MS/MS. The data was collected with Xcalibur 3.0 (Thermo Scientific).

In vivo isotope tracking analysis

A targeted MS/MS method was established for gut bacterial isotope tracking analysis. The scanning cycle consists of one full FT-MS scanning with a mass range of 100-1000 and spectral resolution of 60000, followed by 6 IT-MS/MS scanning events. The MS/MS spectra of 6 targeted epoxy-precursor ions, FA 16:1 (*m/z* = 269.25), FA 17:1 (*m/z* = 283.25), FA 18:1 (*m/z* =297.24), $^{13}C_5$-FA 18:1 (*m/z* = 302.25), FA 19:1 (*m/z* = 311.30), FA 20:1 (*m/z* = 325.30), and D_{17}-FA 18:1 (*m/z* = 314.30), were acquired via ion activation type of CID, isolation width of *m/z* 2.0, NCE of 40, activation Q of 0.250, and activation time of 10.00 ms. The maximum injection time for both full FT-MS and IT MS^n was set at 500 ms with auto-gain-control (AGC) of 1.00e+6 for full FT-MS scan and 3.00e+4 for IT-MS/MS. The data was collected with Xcalibur 3.0 (Thermo Scientific).

C=C isomer quantification

For quantification of lipid C=C isomers, the fraction of a C=C isomer was calculated by dividing the EIC peak area of the diagnostic ions from a specific C=C isomer by the sum of the EIC peak area of the diagnostic ions from each C=C isomer.

The fraction $X_{lipidclass,n(Z\vee E)} = \frac{A_{lipidclass,n(Z\vee E),diagnosticions}}{\sum A_{lipidclass,n(Z\vee E),diagnosticions}}\%$

Calibration curve of FA 18:1 9Z and 9E isomers

The total concentration of FA18:1 was kept at 1 μM with the molar ratio varied ([9E]/[9Z] = 99/1, 90/10, 50/50, 10/90 and 1/99). Each mixture was derivatized with excess *m*CPBA (20 mM) at 50°C for 1 hour and was then analyzed by LC-MS. The calibration curve was constructed by plotting the molar fraction of 9E isomers ([9E]/([9E]+[9Z])%) against the fractions of the summed extracted ion chromatogram(EIC) area of diagnostic ions ($A_{9E}/(A_{9E} + A_{9Z})$ %), where $A_{9E} = [A_{E,\ m/z=155} + A_{E,\ m/z=171}]$, $A_{9Z} = [A_{Z,\ m/z=\ 155} + A_{Z,\ m/z=171}]$, both obtained from the MS/MS channel at *m/z* 297.24. Each point represents a technical triplicate.

Bacteria culture

The bacteria used in this study were purchased from Bioresource Collection and Research Center (BCRC) in Taiwan. The medium for each gut bacteria was listed in supplementary table 1. For broth culture, 0.5 mL stock solution was diluted by 10 mL medium and grew to a stationary phase before lipid extraction. For agar plate culture, the 0.1 mL stock solution was transferred to the agar plate and then grew for 3 days before lipid extraction. The whole process was conducted in the anaerobic workstation (N_2: H_2: CO_2 = 8:1:1) (Whitley DG250, Don Whitley Scientific Limited, England).

In vitro isotope tracking

When the bacteria entered the stationary phase, the bacteria solution was transferred to a 15 mL centrifuge tube and was diluted to O.D. ≈ 0.1-0.2 at 600 nm wavelength by addition of MRS broth /MRS broth with 0.5 % EtOH /MRS broth with 0.18 mM $^{13}C_1$-oleic acid and 0.5 % EtOH. $^{13}C_1$-oleic acid was filtered with 0.22 μm filter (Millex GS filter unit, Merck Millipore, Massachusetts, United States) before spiking into MRS. Each condition was tested in quadruplicate and the 0.500 mL bacteria solution was taken out at different growth time (0 hour, 5 hour, 10 hour, and 24 hour) and 0.1 mL D_{17}-FA18:1 (9Z) (10 μM in ethanol) was added as the internal standard. Then 0.600 mL MTBE and 0.150 mL MeOH were added to the samples and sonicated for 30 minutes. The organic layer was transferred to another centrifuge tube, and then 0.3 mL MTBE and 0.1 mL MeOH was added for the second extraction. After being sonicated for 10 mins, the organic layer was combined and dried in a vacuum concentrator. The 0.1 mL reconstituted solution (ACN/IPA/H_2O = 65/30/5) was added to dissolve the extracts. Then the samples were epoxidated and analyzed by RPLC-MS/MS.

Extraction of gut bacteria lipids

For bacteria growing on an agar plate, the bacterial cells were first scratched into a 1.5 mL micro-centrifuge tube by a cell scraper, and then MTBE/MeOH (v/v = 4/1) 750 μL was added and vortexed for 30 minutes. Then 200 μL ddH_2O was added for phase separation. The sample was then centrifuged for 3 minutes at 12000 rpm, and then the upper organic layer was transferred into another 1.5 mL micro-centrifuge tube. The second extraction was conducted by adding 100 μL ddH_2O, 100 μL MeOH, and 300 μL MTBE and vortexed for 10 minutes. Then the sample was centrifuged at 12000 rpm for 1minute. After centrifuging, all extraction was collected together. The solution was dried in a vacuum concentrator, and then the 0.1 mL reconstituted solution (ACN/IPA/H_2O = 65/30/5) was added to dissolve the extracts. For bacteria growing in broth, 0.5 mL bacteria solution was taken out and 0.1mL D_{17}-FA 18:1 (9Z) (33 μM in MeOH) was added into the solution. Then 400 μL MTBE was added and the solution was sonicated for 30 minutes. Then the organic layer was transferred into another 1.5 mL micro-centrifuge tube. The second extraction was conducted by adding 100 μL MeOH and 300 μL MTBE, and then sonicated for 10 minutes. Then the organic layers were combined, dried, and reconstituted as described above. The reconstituted samples were stored at -80°C before further analysis.

MUFA profiling of gut bacteria lipid extracts

The *m*CPBA reagent (200 mM) was prepared beforehand by dissolving *m*CPBA powders with methanol. The lipid extracts were mixed with *m*CPBA at equal volume, and then the mixture was heated at 50°C for 1 hour. The mixture was then analyzed by RPLC-MS/MS, and the fraction of each isomer was calculated by the corresponding diagnostic ions.

In vivo isotope tracking

To test the effect of gut bacteria on fatty acid isomers *in vivo*, five 10-week female C57BL/6JNarl SPF mice feces and five 12-week female C57BL/6JNarl germ-free mice were gavaged $^{13}C_5$-FA 18:1 9Z (2.7 mg/mL grapeseed oil) at the dose amount of 20 mg per kilogram body weight. Mice feces were collected before and at 6 hours after the intake of the isotope tracer respectively for lipid extraction. (IACUC number: NLAC-107-O-006-R7). The mice model was done by Leeuwenhoek Laboratories Co. Ltd., Taipei, Taiwan (IACUC number: 00169). The feces were lyophilized, ground into powder, and weighed before lipid extraction. Then the internal standard D_{17}-FA 18:1 9Z (33 μM in ethanol) was added at 4.95 μL per milligram of feces. The first extraction was conducted by the addition of MTBE/MeOH (v/v = 4/1) at 37.1 μL per milligram of feces and sonicated

for 1 hour. Then ddH_2O was added at 9.9 µL per milligram of feces for phase separation and the samples were centrifuged at 12000 rpm for 5 minutes. The upper organic layer was collected centrifuged tube and ddH_2O/MeOH/MTBE (v/v/v = 1/1/3) was added into the water layer at 24.8 µL per milligram of feces for the second extraction. The samples were sonicated for 30 minutes and then centrifuged at 12000 rpm for 5 minutes. The organic layers were combined and dried in the vacuum concentrator. Then the reconstituted solution (ACN/IPA/H_2O = 65/30/5) was added at 4.95 µL per milligram of feces. The reconstituted samples were stored at -80 °C before further analysis.

RESULT AND DISCUSSION

The working principle of epoxidation-assisted structural lipidomics in characterizing lipid C=C position and geometry

The working principle was depicted in Figure. 1, with a hypothetical example that considers four isomers differing in C=C position and/or geometry to explain the analytical process. The method exploits *m*CPBA as a derivatization reagent to chemically modify lipid C=C bonds prior to mass spectrometric analysis. *m*CPBA enables stereoselective epoxidation at a C=C bond, forming an epoxide moiety (i.e., a three-membered ring with one oxygen heteroatom) with a preserved *trans*/*cis* geometry. The epoxide moiety is more fragile than C=C, thus allowing direct C=C positional identification by conventional MS/MS (e.g., CID in negative ion mode), a process where a lipid epoxide generates an aldehyde-alkene fragment pair specific to C=C position (Figure. 1b-c). However, the integration of *m*CPBA epoxidation and MS/MS can hardly distinguish between geometrical isomers as they generate identical tandem mass spectra, as observed in our previous study[33].

C=C geometry plays a determinant role in the hydrophobicity of an unsaturated lipid. Generally understood, the formation of the *cis*-C=C bond causes a fatty acyl chain to 'bend', thus decreasing molecular hydrophobicity; in contrast, the formation of *trans*-C=C bond leaves molecular hydrophobicity less changed. Taking advantage of this chemical property, this method exploits reverse-phase liquid chromatography (RPLC) analysis to provide an additional dimension of isomer-differentiating capability other than MS/MS. As further explained by the hypothetical example in Fig. 1b-c, the mixed isomers (epoxy-lipids) are chromatographically separated in RPLC-MS/MS analysis, with their tandem mass spectra continuously recorded overtime. This analytical configuration allows simultaneous identification of C=C geometry and position in two steps. First, C=C position is identified by peak alignment between the lipid and its C=C-position-specific fragments (as measured in MS^1 and MS/MS, respectively). Second, C=C geometry is identified by retention time sequence. Given that a lipid with greater hydrophobicity is exposed to stronger retention in RPLC, a pair of *cis*/*trans* geometrical isomers results in two chromatographic peaks with the "*cis*-to-*trans*" order; that is, the *trans* isomer shows longer retention time than its *cis* isomer.

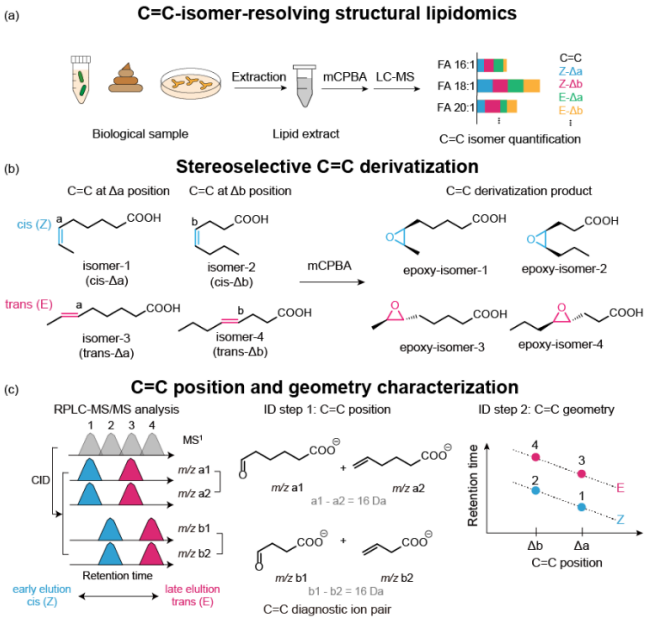

Figure 1. (a) The epoxidation-assisted structural lipidomics workflow. (b) Stereoselective C=C derivatization by *m*CPBA. Unsaturated lipid isomers are derivatized by *m*CPBA, a fast in-solution epoxidation that *trans*forms C=C bonds into epoxides with preserved *trans*/*cis* stereochemistry. (c) The derivatized isomers are analyzed with RPLC-MS/MS and identified for their original C=C position and *trans*/*cis* geometry according to MS/MS diagnostic ion pairs and retention time sequences, respectively. After epoxidation derivatization and subsequently upon tandem mass spectrometry (e.g., CID) in negative ion mode, each C=C isomer yields an aldehyde-alkene fragment pair indicative of the C=C position.

Method validation with lipid isomer standards

The C=C-resolving capability was validated systematically with authentic standards of two main lipid classes, fatty acid and glycerophospholipid. We applied this method to examine a mixture of 14 standards of mono-unsaturated fatty acid (MUFA) that differ in acyl chain length, C=C position, and C=C geometry, including five FA 16:1 isomers (Figure S1a-d), seven FA 18:1 isomers (Figure. 2a-c), and two FA 20:1 isomers (Figure. S1e-f). There were collectively four properties that facilitated the identification of C=C bonds. Taking the FA 18:1 isomer series as an example, we observed (i) epoxidation derivatization generally decreased the hydrophobicity of all C=C isomers, resulting in an overall shorter retention time (Figure. 2a); (ii) the C=C position was pre*cis*ely pinpointed by Δ16-Da fragment pairs in MS/MS spectra (Figure. 2b-c and Figure S2) and by their corresponding fragment chromatograms (Figure. 2a), regardless C=C geometry; (iii) as the C=C position moved further from the carboxylic acid group (i.e., greater Δ number), the retention time decreased (Figure. 2a); (iv) for each pair of geometrical isomers, the *trans* and *cis* forms showed baseline separation and followed the "*cis*-to-*trans*" order in retention time, providing a foundation for robust quantification of geometrical isomers (Figure. 2a). These four observations were also valid for the FA 16:1 and 20:1 isomers (Figure. S1). We further discovered that, for a given series of C=C positional isomers (e.g., FA 18:1 isomers that have *trans*-C=C bonds at different positions), the retention time was numerically linear to the C=C position (Figure. 2d). This mathematical relationship allows a rational C=C identification of an unknown lipid without its commercial or

synthetic standard, which is particularly important during a large-scale screening of lipid isomers. Additionally, the limit of detection (LOD) of identifying C=C-diagnostic ions as assessed by FA 18:1 9E was approximately at the nM level, thus allowing the identification of geometrical isomers of low abundance (Figure. 2e).

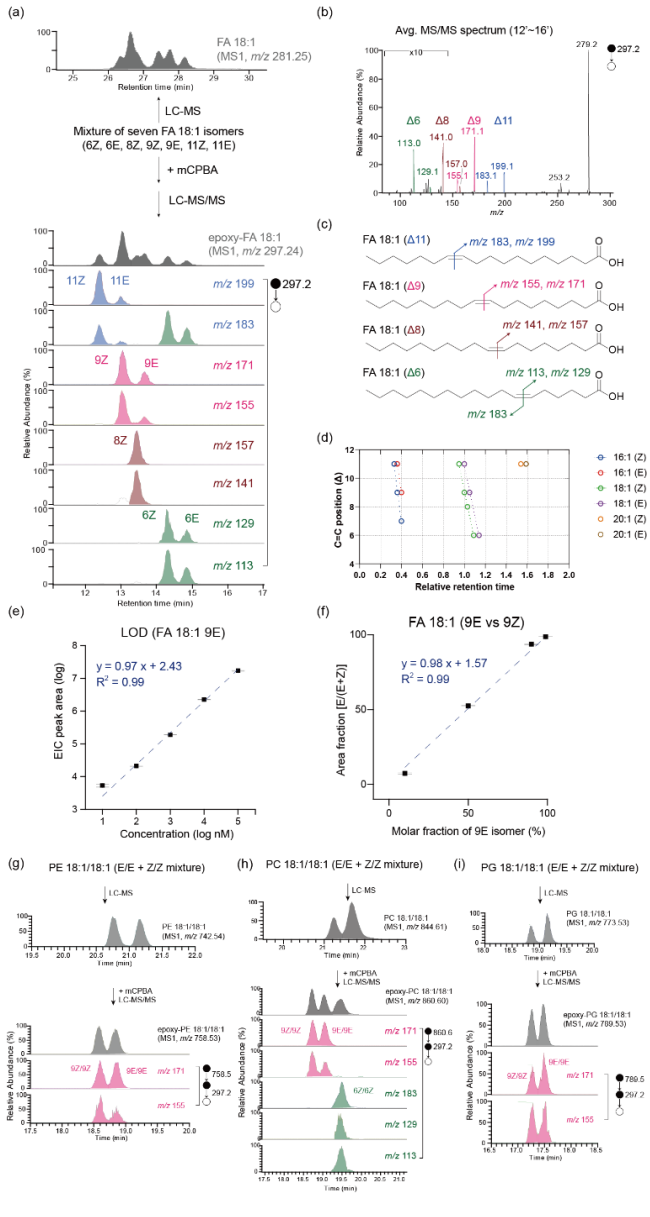

Figure 2. (a-c) A standard mixture consisting of FA 18:1 isomers (unequal concentrations) was examined to demonstrate the analytical capability of identifying C=C position and geometry. (a) The extracted ion chromatogram (EIC) of non-derivatized and epoxidation-derivatized FA isomers. The same chromatographic parameters were used. (b) The representative tandem mass spectrum of epoxidation-derivatized isomers. Fragment pairs indicative of C=C positions were highlighted. (c) Fragmentation scheme. (d) Retention time index of FA isomer standards. Linear fitting was performed on each series of C=C positional isomers with identical acyl chain lengths and cis/trans geometry. (e) Limit of detection of the C=C-diagnostic ion pairs of FA 18:1 9E. (f) Calibration curve for *cis*/*trans*-isomer quantification of FA 18:1 (9Z versus 9E). In (e-f), each point and error bar represent the means and the standard deviation calculated by technical triplicates. In (e-f), area refers to the summed EIC peak area of the C=C-diagnostic ion pair in RPLC-MS/MS analysis. (g-i) The EICs of the phospholipid epoxides and the diagnostic ions. In (e-f), each point and error bar represent the means and the standard deviation calculated by technical triplicates.

To validate quantification capability, we examined a mixture with FA 18:1 9Z and 9E isomers of varied ratios at a fixed total isomer concentration (described in material and method). The built calibration curve (Figure. 2f) showed good linearity (R^2 = 0.99) between C=C-diagnostic ion abundance (y-axis) and isomer composition (x-axis). Meanwhile, the slope of the fitted calibration line (0.98) was close to 1, implying that the ratio of C=C-diagnostic ion abundance served as a reliable estimation of the geometrical isomer composition. Besides FA, the method was generally applicable to identify C=C position and geometry in FA-constituting phosphoglycerolipids, such as phosphoethanolamine (PE), phosphatidylcholine (PC), and phosphatidylglycerol (PG) (Figure. 2g-i). Similar quantitative results were also obtained by analyzing phospholipid geometric isomers mixture (Figure. S3). In our previous study, we demonstrated the feasibility of measuring the composition of positional isomers by C=C-diagnostic ion abundance[33]. Combining together, we suggest this method provides an empirical approach to quantify the composition of both positional and geometric C=C isomers of a given unsaturated lipid species, a chemical information that complements traditional lipidomics results. While C=C identification of poly-unsaturated lipid could be challenging due to multiple derivatization products, it remained possible to assign C=C geometry and position by directly comparing between isomer spectra (as exemplified by FA 18:2 geometrical and positional isomers in Figure. S4).

Lipid C=C isomers analysis of gut bacterial lipid extracts

To demonstrate the potential of this method to analyze C=C isomers in biological samples, we analyzed the lipid extracts from different common gut bacteria (Supplementary table 1). The analysis workflow was depicted in Figure. 1a. We initiated the analysis by employing data-dependent acquisition (DDA) on samples without epoxidation. This enabled us to obtain a list of unsaturated lipid candidates for epoxidation in each sample. The relative abundance of saturated fatty acid and monounsaturated fatty acid with carbon chains ranging from 16 to 20 in the gut bacterial extracts was determined by the MS^1 EIC peak area, while their C=C positions and geometries remained unknown (Figure. 3a). Subsequently, upon epoxidation, multiple peaks of C=C diagnostic ions were observed in MS^2 EICs (Figure. S5), which allowed us to determine the C=C position and geometry and calculate the relative abundance of the C=C isomers (Figure. 3b and Figure. S6). Also, the relative retention time of each peak of diagnostic ions was consistent with the standards (Figure. 4a and Supplementary table 2). Notably, more than 30 C=C isomers were identified in the gut bacterial extracts for the unsaturated fatty acid we targeted, namely FA16:1-FA20:1 (Figure. 4b). These results not only suggested that our method significantly increased the identification number, but also showed the potential of gut bacteria to generate C=C isomers. In contrast, the number of phospholipid C=C isomers identified in the bacterial extracts was quite fewer than that of unsaturated fatty acid. More precisely, the EICs for the C=C diagnostic showed one peak in most cases of unsaturated phospholipid, which means only one of the geometric isomers was observed (Figure. S7 & Figure. S8).

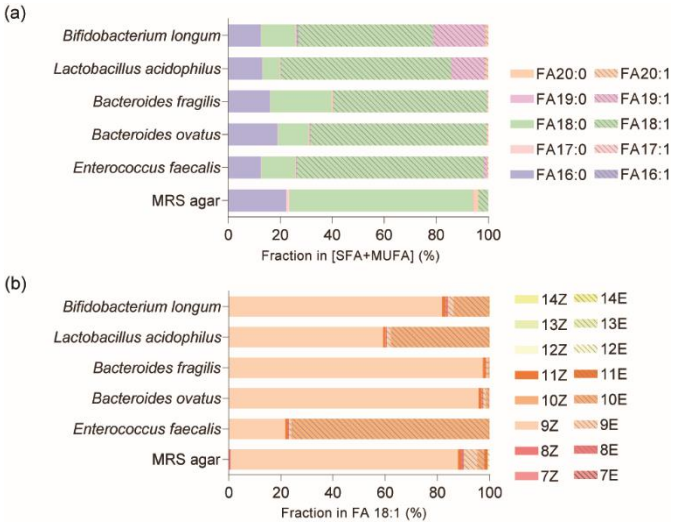

Figure 3. Saturated and unsaturated fatty acid composition of the gut bacteria cultured in MRS. (a) The composition of fatty acids (saturated fatty acid (SFA) and mono-unsaturated fatty acid (MUFA), characterized at species level) in the lipid extracts from gut bacteria cultured by MRS agar. (b) The C=C isomer composition of FA 18:1 with C=C position and geometry characterized.

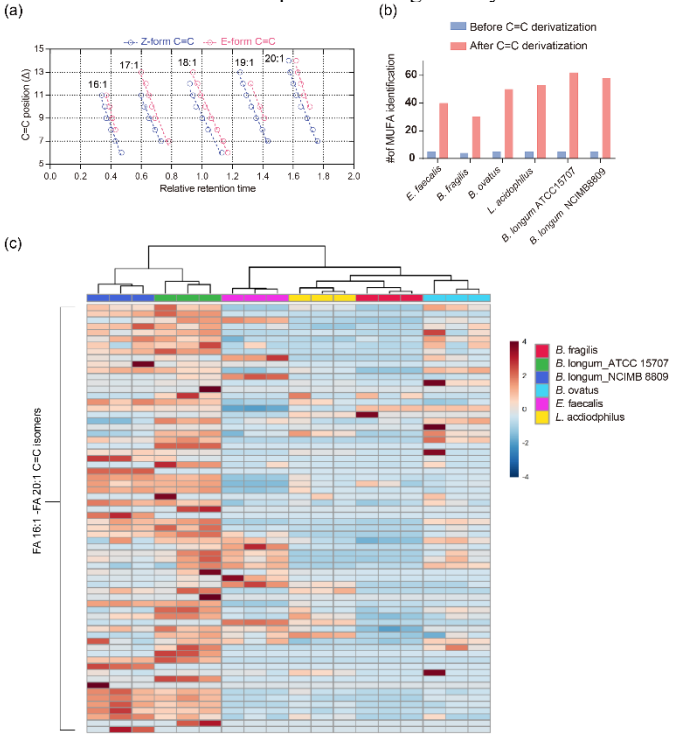

Figure 4. Applying the epoxidation-assisted structural lipidomics to investigate gut bacterial lipid isomerism. (a) Retention time index of the identified bacterial isomers. Linear fitting was performed on each series of C=C positional isomers with identical acyl chain lengths and *cis*/*trans* geometry. Data in (a) represents the means calculated from biological triplicates. (b) The identification number of MUFA before C=C derivatization (with C=C position and geometry unresolved) and that of the MUFA C=C isomers species corresponding to the unresolved MUFA species after C=C derivatization (with C=C position and geometry resolved) (c) Clustering analysis of gut bacteria by the FA C=C isomers profile.

To ensure the reproducibility of this method, we cultured each gut bacteria in MRS in triplicate and obtained their C=C isomer profiles. The heatmap profile showed the reproducibility of our method and that the *B. longum* ATCC 15707 and *B. longum* NCIMB 8809 was clustered together, which indicated a similar C=C isomer composition for the same gut bacteria species (Figure. 4c and Figure. S9). Principle component analysis (PCA) further indicated that different gut bacteria species could be classified based on their C=C isomer profile (Figure. S10). Notably, though the saturated and unsaturated fatty acid composition of these gut bacteria was similar (Figure. 3a), the C=C isomers composition was quite different (Figure. 3b and Figure. S6). In addition to the common unsaturated fatty acids such as FA 18:1 9Z, FA 18:1 11Z and FA 20:1 11Z, we also identified other C=C isomers with relatively low abundance which were seldom reported. Interestingly, we found that FA 18:1 10E was also a common unsaturated fatty acid C=C isomer in the bacterial extracts with relatively high abundance in *trans*-isomers (Figure. 3b and Figure. S6). In the case of *E. faecalis*, the abundance was even higher than FA 18:1 9Z (Figure. 3b) and accounted for over 50% among the FA 18:1 C=C isomers, which indicated that FA 18:1 10E was the C=C isomer generated by gut bacteria. We also analyzed lipid extracts from the gut bacteria cultured in TSA medium and profiled the C=C isomers composition. The results suggested that the C=C isomers composition of the same gut bacteria species cultured in different medium was quite different, which indicated that the C=C isomers composition of the gut bacteria was media-dependent (Figure. S6 and Figure. S11). This may be because different growth conditions affected gut bacteria's ability to generate C=C isomers or some C=C isomers were absorbed from the medium.

Integration with isotope tracking experiment to deduce bacterial C=C isomer origin

The notably high abundance of FA 18:1 10E in gut bacterial lipid extracts captured our attention, motivating us to further delve deeper into its biochemical origin. Yet this observation might be attributed simply to bacterial uptake and accumulation of medium contents, although FA 18:1 10E exhibited limited prevalence in media as quantified above. To test whether FA 18:1 10E is a result of biotransformation activities by gut bacteria, we conducted an isotope-tracking experiment. This approach involved culturing bacteria in the presence of an isotope-labelled compound as biotransformation substrate and assessing whether the isotope-labeled atom is present in the target product, which in this case is FA 18:1 10E. Herein, we tested three common fatty acids, namely $^{13}C_1$-FA 18:0, $^{13}C_1$-FA 16:0, and $^{13}C_1$-FA 18:1 9Z, generally recognized as precursors for downstream unsaturated lipid synthesis (Figure 5a). Following experiments with *B. longum*, we discovered that the supplementation of $^{13}C_1$-FA18:1 9Z, but not $^{13}C_1$-FA 18:0 or $^{13}C_1$-FA 16:0 (Figure 5b-c), specifically contributed to the isotope enrichment of FA 18:1 10E, as indicated by an elevated abundance of the ^{13}C isotope of FA18:1 9Z (referring to 10E-specific diagnostic MS^2 fragments, *m/z* 186 and *m/z* 170, in Figure 5a) in association with a reduction of the precursor due to bacterial metabolism (Figure 5c). Isotope enrichment of other FA 18:1 isomer was not observed, implying the specificity of the 9Z-to-10E conversion. Similar results were obtained when performing the experiment with two other selected gut species, *E. faecalis*, and *L. acidophilus* (Figure 5d). Overall, these findings suggest that these gut bacteria generate FA18:1 10E through an unreported, putative isomeric biotransformation pathway using FA18:1 9Z

as the substrate (Figure 5e), whereas the detailed mechanism is currently under investigation.

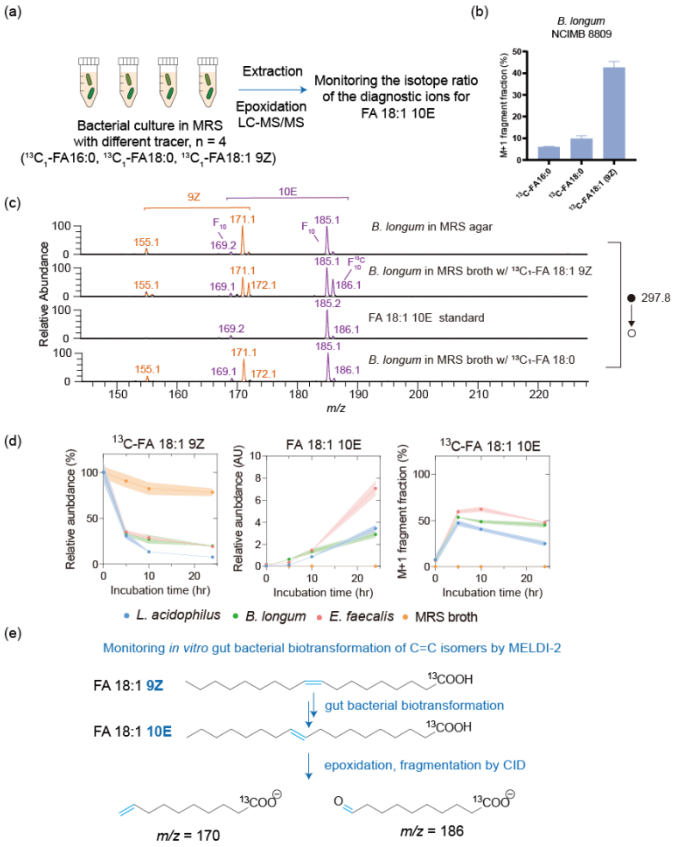

Figure 5. *In vitro* gut bacterial isomerization of FA 18:1 (9Z) into FA 18:1 (10E). (a) The experiment scheme. (b) The M+1 fraction of the diagnostic ions for FA 18:1 10E in the lipid extracts from *B. longum*. The M+1 fragment fraction was calculated by (A_{170} + A_{186})/(A_{169} + A_{185} + A_{170} + A_{186}) (c) The MS/MS spectra of FA 18:1 epoxides in the lipid extracts from *B. longum*. (d) The abundance of $^{13}C_1$-FA 18:1 (9Z), FA 18:1 (10E), and $^{13}C_1$-FA 18:1 (10E) in the lipid extracts at different incubation times. Data represent the means calculated from biological triplicates (e) The proposed putative isomerization mechanism and fragmentation mechanism.

We have unraveled that gut bacterial lipid extracts contained a diverse consortium of lipid C=C isomers. These observed bacterial C=C isomers are rarely discussed in the context of mammalian lipidomics studies, possibly owing to analytical limitations, yet still raising the question of whether gut bacterial lipidome, as well as the bacterial lipid metabolic activities, might be an *in vitro* experiment defects and lost its relevance when considering gut bacteria in the host gastrointestinal track. We thus attempted to address this challenge by further applying a similar isotope-tracking experiment to animal experiments. As a pilot study, we utilized the germ-free mouse model (GF), in comparison to the specific-pathogen-free mouse (SPF), to determine whether the presence of gut bacteria played a role in the FA 18:1 9Z-to-10E conversion (Figure 6a). After 6 hr since oral administration of an isotope-labeled FA 18:1 9Z as a metabolic tracer, we performed target quantification of fecal FA 18:1 C=C isomers and found significantly higher amounts of isotope-labeled 10E isomer in SPF mice but not detectable in GF mice (Figure 6b-c and Figure S12). Also, the amount of un-labeled FA 18:1 10E was higher in SPF mice than GF mice (Figure S13.) Interestingly, we also observed a higher amount of tracer retained in SPF mouse feces (Figure S13), implying that the metabolism of the 9Z isotope tracer might be faster in GF mice and yet not reflect on bacteria-independent production of the 10E isomer. Overall, our preliminary results suggest that the presence of bacteria might be essential for the production of FA 18:1 10E in the gut and that bacterial biotransformation of FA 18:1 9Z to its 10E isomer might happen in the gut. While this conclusion requires further validation through rigorous experiments involving bacterial genetics and gnotobiology to identify responsible bacterial species and enzymes, we foresee that integrating our structural lipidomics workflow would be complement the elucidation of elucidate gut bacterial metabolic pathway by offering an in-depth level of lipid C=C isomer quantification.

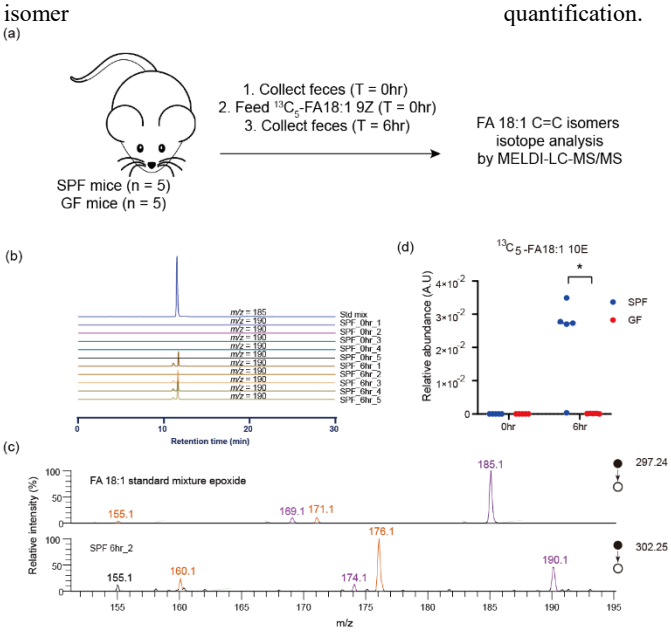

Figure 6. *In vivo* isotope tracking with $^{13}C_5$-FA 18:1 9Z. (a) Experiment scheme. (b) The MS^2 EICs of the diagnostic ion for FA 18:1 10E and $^{13}C_5$-FA 18:1 10E. (*m/z* = 185: monoisotopic diagnostic ions for FA 18:1 10E, CID @ *m/z* = 297.24. *m/z* = 190: $^{13}C_5$-labelled diagnostic ions, CID @ *m/z* = 302.25). (Std mix: The standard mixture of FA 18:1 9Z and FA 18:1 10E. SPF_ahr_b: SPF: SPF mice feces, a: Time point that feces collected after feeding isotope, b: number of mice (n = 5). (c) The MS^2 spectra of FA 18:1 epoxide. (d) The relative quantification of $^{13}C_5$-FA 18:1 10E (normalized to the internal standard).

CONCLUSION

In this study, we developed a novel, user-friendly method for identifying and quantifying unsaturated lipid C=C isomers. We validated the method by analyzing artificial standard mixture and gut bacterial lipid extracts. Furthermore, we successfully identified a series of positional and geometric unsaturated C=C isomers and profiled the isomer composition of the gut bacterial lipid extracts with the C=C position and geometry characterized. Notably, the in vivo and in vitro isotope tracking experiments suggested an unreported gut bacterial biotransformation pathway where the FA 18:1 9Z was converted into FA 18:1 10E. Given the effect of trans unsaturated fatty acid on human health, the pathway was potentially another important interaction between gut bacteria and host

ASSOCIATED CONTENT

Supporting Information

Supplementary methods and figures (.docx)
Supplementary table (.xlsx)
EpoxyFinder software: ZIP

AUTHOR INFORMATION

Corresponding Author

Cheng-Chih Hsu*
Email: ccrhsu@ntu.edu.tw
Phone: +886-2 3366-3844

ORCID

Kai-Li Chen: 0009-0000-5627-2564
Ting-Hao Kuo: 0000-0001-5130-0570
Cheng-Chih Hsu: 0000-0002-2892-5326

Present Addresses

‡ European Molecular Laboratory, Heidelberg, Germany.

Author Contributions

K.-L.C. and T.-H.K. designed and conducted the experiment.
K.-L.C. and T.-H.K. wrote the paper.
C.-C.H. supervised the study.
‖ These authors contributed equally.

Notes

The authors declare no conflict of interest.

ACKNOWLEDGMENT

This research was supported by Ministry of Science and Technology (MOST), R.O.C. (Grants MOST 108-2636-M-002-008-, 109-2636-M-002-005-, and 110-2636-M-002-014-) T.-H. K. acknowledges "The Program of Research Performance Enhancement via Students Entering PhD Programs Straight from an Undergraduate/Master's Program" from National Taiwan University. The instrument support from National Taiwan University Mass Spectrometry Platform was acknowledged.

REFERENCES

(1) Thursby, E.; Juge, N. *Biochemical Journal* **2017**, 474 (11), 1823-1836.
(2) Fan, Y.; Pedersen, O. *Nature Reviews Microbiology* **2021**, 19 (1), 55-71.
(3) Wu, H.-J.; Wu, E. *Gut Microbes* **2012**, 3 (1), 4-14.
(4) Lindell, A. E.; Zimmermann-Kogadeeva, M.; Patil, K. R. *Nature Reviews Microbiology* **2022**, 20 (7), 431-443.
(5) Nicholson, J. K.; Holmes, E.; Kinross, J.; Burcelin, R.; Gibson, G.; Jia, W.; Pettersson, S. *Science* **2012**, 336 (6086), 1262-1267.
(6) Donia, M. S.; Fischbach, M. A. *Science* **2015**, 349 (6246), 1254766.
(7) Zimmermann, M.; Zimmermann-Kogadeeva, M.; Wegmann, R.; Goodman, A. L. *Nature* **2019**, 570 (7762), 462-467.
(8) Heaver, S. L.; Johnson, E. L.; Ley, R. E. *Current Opinion in Microbiology* **2018**, 43, 92-99
(9) Sugimoto, Y.; Camacho, F. R.; Wang, S.; Chankhamjon, P.; Odabas, A.; Biswas, A.; Jeffrey, P. D.; Donia, M. S. *Science* **2019**, 366 (6471), eaax9176.
(10) Bae, M.; Cassilly, C. D.; Liu, X.; Park, S.-M.; Tusi, B. K.; Chen, X.; Kwon, J.; Filipčík, P.; Bolze, A. S.; Liu, Z.; Vlamakis, H.; Graham, D. B.; Buhrlage, S. J.; Xavier, R. J.; Clardy, J. *Nature* **2022**, 608 (7921), 168-173.
(11) Brial, F.; Le Lay, A.; Dumas, M.-E.; Gauguier, D. *Cellular and molecular life sciences* **2018**, 75 (21), 3977-3990.
(12) Morrison, D. J.; Preston, T. *Gut Microbes* **2016**, 7 (3), 189-200.
(13) Li, Houkai, Jiaojiao He, and Wei Jia. *Expert opinion on drug metabolism & toxicology* 12.1 (**2016**): 31-40.
(14) Tsiantas, K.; Konteles, S. J.; Kritsi, E.; Sinanoglou, V. J.; Tsiaka, T.; Zoumpoulakis, P. *International Journal of Molecular Sciences* **2022**, 23 (8), 4070.
(15) Kimura, I.; Ozawa, K.; Inoue, D.; Imamura, T.; Kimura, K.; Maeda, T.; Terasawa, K.; Kashihara, D.; Hirano, K.; Tani, T.; Takahashi, T.; Miyauchi, S.; Shioi, G.; Inoue, H.; Tsujimoto, G. *Nature Communications* **2013**, 4 (1), 1829.
(16) Morozumi, S.; Ueda, M.; Okahashi, N.; Arita, M. *Biochimica et Biophysica Acta (BBA) - Molecular and Cell Biology of Lipids* **2022**, 1867 (3), 159110.
(17) Schoeler, M.; Caesar, R. *Reviews in Endocrine and Metabolic Disorders* **2019**, 20 (4), 461-472.
(18) Keweloh, H.; Heipieper, H. J. *Lipids* **1996**, 31 (2), 129-37.
(19) Heipieper, H. J.; Loffeld, B.; Keweloh, H.; de Bont, J. A. M. *Chemosphere* **1995**, 30 (6), 1041-1051.
(20) Rustam, Y. H.; Reid, G. E. *Analytical Chemistry* **2018**, 90 (1), 374-397.
(21) Hu, T.; Zhang, J. L. *Journal of Separation Science* **2018**, 41 (1), 351-372.
(22) Cimen, I.; Yildirim, Z.; Dogan, A. E.; Yildirim, A. D.; Tufanli, O.; Onat, U. I.; Nguyen, U.; Watkins, S. M.; Weber, C.; Erbay, E. *Molecular Metabolism* **2019**, 28, 58-72.
(23) Belury, M. A. *The Journal of Nutrition* **2002**, 132 (10), 2995-2998.
(24) Calder, P.; Grimble, R. *European Journal of Clinical Nutrition* **2002**, 56 (3), S14-S19.
(25) Mozaffarian, D.; Pischon, T.; Hankinson, S. E.; Rifai, N.; Joshipura, K.; Willett, W. C.; Rimm, E. B. *The American Journal of Clinical Nutrition* **2004**, 79 (4), 606-612.
(26) Kelley, N. S.; Hubbard, N. E.; Erickson, K. L. *The Journal of Nutrition* **2007**, 137 (12), 2599-2607.
(27) Porta Siegel, T.; Ekroos, K.; Ellis, S. R. *Angewandte Chemie International Edition* **2019**, 58 (20), 6492-6501.
(28) Baba, T.; Campbell, J. L.; Le Blanc, J. C. Y.; Baker, P. R. S. *Analytical Chemistry* **2017**, 89 (14), 7307-7315.
(29) Williams, P. E.; Klein, D. R.; Greer, S. M.; Brodbelt, J. S. *Journal of the American Chemical Society* **2017**, 139 (44), 15681-15690.
(30) Takahashi, H.; Shimabukuro, Y.; Asakawa, D.; Yamauchi, S.; Sekiya, S.; Iwamoto, S.; Wada, M.; Tanaka, K. *Analytical Chemistry* **2018**, 90 (12), 7230-7238.
(31) Pham, H. T.; Ly, T.; Trevitt, A. J.; Mitchell, T. W.; Blanksby, S. J. *Analytical Chemistry* **2012**, 84 (17), 7525-7532.
(32) Ma, X.; Xia, Y. *Angewandte Chemie International Edition* **2014**, 53 (10), 2592-2596.
(33) Kuo, T.-H.; Chung, H.-H.; Chang, H.-Y.; Lin, C.-W.; Wang, M.-Y.; Shen, T.-L.; Hsu, C.-C. *Analytical Chemistry* **2019**, 91 (18), 11905-11915.
(34) Tang, S.; Cheng, H.; Yan, X. *Angewandte Chemie International Edition* **2020**, 59 (1), 209-214.
(35) Thomas, M. C.; Mitchell, T. W.; Blanksby, S. J. *Journal of the American Chemical Society* **2006**, 128 (1), 58-59.
(36) Zhang, J. I.; Tao, W. A.; Cooks, R. G. *Analytical Chemistry* **2011**, 83 (12), 4738-4744.

(37) Hirtzel, E.; Edwards, M.; Freitas, D.; Yan, X., Aziridination-assisted mass spectrometry of nonpolar lipids with isomeric resolution. **2022**.
(38) Adhikari, S.; Zhang, W.; Xie, X.; Chen, Q.; Xia, Y. *Analytical Chemistry* **2018**, 90 (8), 5239-5246.
(39) Song, C.; Gao, D.; Li, S.; Liu, L.; Chen, X.; Jiang, Y. *Analytica Chimica Acta* **2019**, 1086, 82-89.
(40) Leaptrot, K. L.; May, J. C.; Dodds, J. N.; McLean, J. A. *Nature Communications* **2019**, 10 (1), 1-9.
(41) Kyle, J. E.; Zhang, X.; Weitz, K. K.; Monroe, M. E.; Ibrahim, Y. M.; Moore, R. J.; Cha, J.; Sun, X.; Lovelace, E. S.; Wagoner, J. *Analyst* **2016**, 141 (5), 1649-1659.
(42) Ecker, J.; Scherer, M.; Schmitz, G.; Liebisch, G. *Journal of Chromatography B* **2012**, 897, 98-104.
(43) Xie, X.; Xia, Y. *Analytical Chemistry* **2019**, 91 (11), 7173-7180.
(44) Feng, G.; Gao, M.; Wang, L.; Chen, J.; Hou, M.; Wan, Q.; Lin, Y.; Xu, G.; Qi, X.; Chen, S. *Nature Communications* **2022**, 13 (1), 2652.
(45) Liebisch, G.; Vizcaíno, J. A.; Köfeler, H.; Trötzmüller, M.; Griffiths, W. J.; Schmitz, G.; Spener, F.; Wakelam, M. J. *Journal of lipid research* **2013**, 54 (6), 1523-1530.